Mixed-Mode Oscillations in Complex Plasma Instabilities

Maxime Mikikian, Marjorie Cavarroc, Lénaïc Couëdel, Yves Tessier, Laifa Boufendi

Mixed-Mode Oscillations in Complex Plasma Instabilities

Maxime Mikikian,* Marjorie Cavarroc, Lénaïc Couëdel, Yves Tessier, and Laïfa Boufendi
GREMI, Groupe de Recherches sur l'Energétique des Milieux Ionisés, UMR6606, CNRS/Université d'Orléans, 14 rue d'Issoudun, BP6744, 45067 Orléans Cedex 2, France
(Dated: June 10, 2008)

Instabilities in dusty plasmas are frequent phenomena. We show that some instabilities can be described by mixed-mode oscillations often encountered in chemical systems or neuronal dynamics and studied through dynamical system theories. The time evolution of these instabilities is studied through the change in the associated waveform. Frequency and interspike interval are analyzed and compared to results obtained in other scientific fields concerned by mixed-mode oscillations.

PACS numbers: 52.27.Lw, 52.35.-g, 52.25.Gj, 05.45.-a

Solid dust particles from a few nanometers to centimeters are often present in plasmas and are at the origin of a wide variety of new phenomena. Plasmas containing dust particles are called dusty or complex plasmas. These media are encountered in many environments such as astrophysics, industrial processes and fusion devices. Dust particles can come from regions in the plasma vicinity or can be formed in the plasma due to the presence of molecular precursors. In most cases, they acquire a negative charge by attaching plasma free electrons. In plasma reactors, dust clouds are often characterized by a central dust-free region. This region, usually named "void" [1–6], is considered to be maintained by an equilibrium between inward electrostatic and outward ion drag forces. Under certain conditions, this equilibrium can be disturbed, resulting in self-excited low frequency oscillations of the void size. The obtained instability, consisting of successive contractions and expansions of the void, is named "heartbeat" [1, 4, 7, 8] due to its apparent similarity with a beating heart. Nevertheless, the dust cloud behavior is more complex than it could be supposed [7, 8]. This self-excited instability can stop by its own through an ending phase characterized by failed contractions that appear more and more numerous as the end approaches. The phenomena sustaining the instability evolve progressively until a new stable state is reached. This phase can be studied by analyzing the discharge current or the plasma glow emission. These signals have a well-defined shape that seems similar to mixed-mode oscillations (MMOs).

MMOs are complex phenomena consisting of an alternation of a varying number of small amplitude oscillations in between two larger ones (also named spikes). Small and large amplitude oscillations are often considered as, respectively, subthreshold oscillations and relaxation mechanisms of the system. These MMOs are encountered in a wide variety of fields. In chemistry, reaction kinetics can take the form of MMOs [9, 10] like in the intensively studied Belousov-Zhabotinskii reaction [11, 12]. In natural sciences, MMOs are the subject of an intense research [13–15] since their observation in the Hodgkin-Huxley model of neuronal activity [15, 16]. In this context, they are strongly related to spiking and bursting activities in neurons [17, 18]. In plasma physics, MMOs have been reported in dc glow discharge [19, 20] but to the best of our knowledge, no evidence of MMOs in dusty plasmas have been reported yet. Because of the broad diversity of scientific domains concerned by MMOs, they induced a lot of researches and several approaches have been explored. These studies are based on dynamical system theories, like for example canards [13, 15, 21], subcritical Hopf-homoclinic bifurcation [16, 22] or Shilnikov homoclinic orbits [23, 24].

In this Letter, we report for the first time on the existence of MMOs in dusty plasmas. An example is analyzed and its main characteristics, typical frequencies and evolution of interspike interval, are explored. Particular attention is paid to the evolution of the number of small amplitude oscillations in between consecutive spikes. We thus underline very close similarities with typical MMOs observed in neuronal activity and chemistry.

Experiments are performed in the PKE-Nefedov reactor [2, 25]. A capacitively coupled radiofrequency (rf at 13.56 MHz) discharge is created between two planar parallel electrodes. The static argon pressure is comprised between 0.5 and 1.6 mbar and the applied rf power is around 2.8 W. Dust particles are grown by sputtering a polymer layer deposited on the electrodes and constituted of previously injected melamine formaldehyde dust particles. A few tens of seconds after plasma ignition, a three-dimensional dense cloud of visible grown dust particles (size of a few hundreds of nanometers) is formed. This observation is performed by laser light scattering with standard CCD cameras. The discharge current (related to electron density) is measured on the bottom electrode. Plasma emission in the center is recorded thanks to an optical fiber with a spatial resolution of a few millimeters [8]. These two diagnostics give rather similar results and are used to characterize the ending phase of the heartbeat instability. When void contraction occurs, a high amplitude peak is observed in the signals [8]. Failed void contractions appear as small amplitude oscillations i.e. failed peaks. The first two oscillations in Fig. 1(a) are representative of a typical fully developed heartbeat signal [7] without any failed peak. The

observed shape is the one used as reference, with a main peak corresponding to the fast contraction and a slowly increasing signal (like a shoulder) during the slow void reopening [8]. Then, a transition between this regime and a regime with one failed contraction (arrow in Fig. 1(a)) occurs. At the instant where a large amplitude oscillation is expected, a decrease in the signal occurs. The spike occurrence is then delayed. A similar behavior is obtained in the optical signal, as observed in Fig. 1(b) for a transition between one and two failed peak regimes. Signal shape clearly corresponds to typical MMOs and is remarkably similar to waveforms measured or modeled in chemical systems [9, 10, 12, 24] or in neuronal dynamics [13, 15, 18, 26, 27]. For the sake of simplicity, classical notation for MMOs [9, 12] will be used in the following. Thus, a pattern characterized by L high amplitude oscillations and S small amplitude ones will be noted L^S. As an example, Fig. 1(a) is a transition between 1^0 and 1^1 states, whereas Fig. 1(b) corresponds to a 1^1-1^2 transition. A closer look to this last transition is shown in Fig. 1(c) where the first 1^2 state is superimposed on the last 1^1 state. A vertical dotted line marks the place where signals differ. As it can be observed, signals are nearly identical until this time and no clear indication announces this next change. In dynamical systems, noise can induce drastic changes in system behavior. In the present study, due to a low signal to noise ratio, analyses cannot be performed on raw data. Thus, data in Fig. 1 have been processed using wavelet techniques (checking that no signal distortion was added) in order to remove noise and thus its effect will not be investigated.

As the similarity between our signals and MMOs is established, a more complete study can be performed. For that purpose, electrical signal evolution has been recorded until the complete end of the instability. A typical sequence is shown in Fig. 2(a). The signal mean value

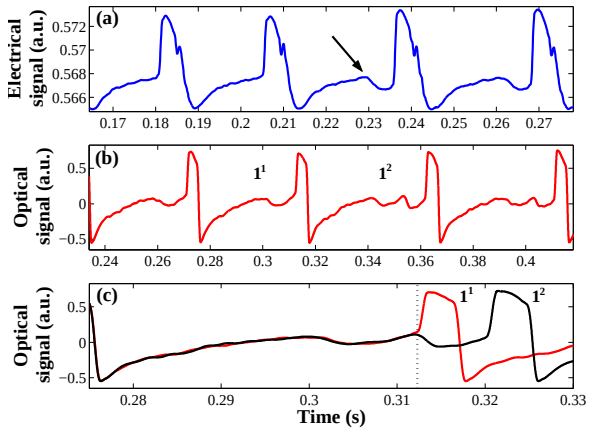

FIG. 1: (color online). (a) Electrical signal with a transition between 1^0 and 1^1 states (arrow: failed peak). (b) Optical signal with a transition between 1^1 and 1^2 states. (c) Superimposition of the two consecutive states shown in (b).

is almost constant and the instability consists of a succession of high amplitude spikes separated by an interspike interval (ISI) increasing as one goes along. As in Fig. 1, low amplitude oscillations appear in between these spikes giving the classical shape of MMOs. The increase in the ISI is thus a consequence of the occurrence of more and more failed peaks. As an example, the insert in Fig. 2(a) shows a 1^4-1^5 transition (this time series starts during the 1^3 state). Just after the transition, the memory that a transition occurred is visible. Indeed, the new failed peak (Fig. 2(a) insert) has a higher amplitude than the other ones, keeping partly the characteristics of a spike. Then, its amplitude decreases during the next few patterns until reaching the same amplitude as the other failed peaks. These MMOs can be also characterized by their corresponding phase space. Figures 2(b)-(c) are respectively 3D and 2D phase spaces of a representative part of the time series presented in Fig. 2(a). To obtain these attractors, an appropriate time delay τ has been calculated using the mutual information method proposed in [28] in the framework of the Belousov-Zhabotinskii reaction. The main large trajectory in phase space corresponds to the large amplitude variation during spikes. A smaller loop (indicated by an arrow labeled 1) corresponds to a short additional peak sometimes observed on the right part of the main spikes [7, 8]. This phenomenon is observed in Fig. 1(a) and does not alter the present study. Small amplitude oscillations are represented by loops in a tiny region indicated by an arrow labeled 2 (Figs. 2(b)-(c)). In this region, the number of loops corresponds to the number of failed peaks (3 loops for the 1^3 state for example) like observed in [15]. The analysis through ISIs is often used in neuroscience for characterizing neural activity [18, 29]. Figure 2(a) shows that the ISI increases by

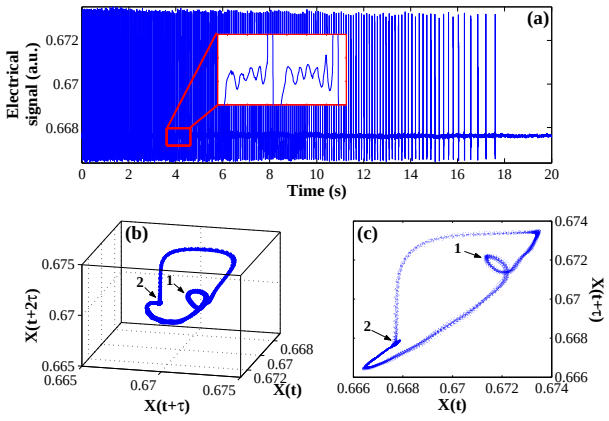

FIG. 2: (color online). (a) Evolution of the electrical signal during the instability ending phase. The insert is a zoom of a transition between 1^4 and 1^5 states. Corresponding phase space is represented in (b) 3D and (c) 2D. Arrows labeled 1 and 2 show respectively the loop due to the additional peak observed on the right hand side of spikes (see Fig. 1(a)) and the region containing the loops corresponding to failed peaks.

the progressive addition of failed peaks until the instability stops. This behavior is better observed by performing a spectrogram, i.e. a time resolved fast Fourier transform (FFT) of this time series (Fig. 3(a)). This analysis clearly shows a step-by-step decrease of the characteristic frequencies until no more oscillations are observed (at ~ 17.7 s). The main frequency corresponding to the spike occurrence is indicated by an arrow labeled 1. Because of the shape of the time series, harmonics are also obtained. Figure 3(a) clearly shows that the frequency jumps become smaller as time increases. Moreover, the duration of a given L^S state decreases with time. These last two properties are also brought to the fore by performing a global FFT of the time series (Fig. 3(b)). Clearly separated peaks are observed, confirming the step-by-step evolution of the frequency. The main peaks are located at $20.5, 17.5, 15.1, 13.3$ and 11.8 Hz. Their amplitude is proportional to the duration of each L^S state. As in Fig. 3(a), it is observed that this duration decreases with time (as the frequency). The amplitude of the first peak at 20.5 Hz is not representative because the time series started to be recorded during the 20.5 Hz phase (1^3 state) and part of this phase is thus missing. Another correlation that can be made with Fig. 3(a), is the decrease of the frequency jumps. Indeed, the frequency jumps are equal to $\Delta f = 3, 2.4, 1.8$ and 1.5 Hz. Finally, Fig. 3(a) gives also the frequency of the failed peaks (arrow labeled 2). It is interesting to note that this frequency does not strongly evolve but only slightly decreases with time (variation of about 10%).

In order to improve the analysis of ISI, the occurrence time of each spike is deduced from the time series presented in Fig. 2(a). Spike position is obtained by detecting points exceeding a correctly chosen threshold. The direct time evolution of the ISI can thus be obtained as shown in Fig. 4(a) (blue dots). A very clear step-by-step behavior, as in [14, 16], is obtained with ISIs varying from ~ 0.05 s (~ 20.5 Hz, 1^3 state) to ~ 0.4 s (~ 2.5 Hz, 1^{40} state). Each step corresponds to the occurrence of a new failed peak, i.e. transition from a L^S to a L^{S+1} state. Close to the end of the instability (after 15 s), the system evolves faster and faster with transitions between L^S and L^{S+n} states with n increasing from 2 to 5. The global time dependence (without taking into account the steps) of ISI evolves as $a+b/(t_0-t)$ as in [16, 22]. Parameters a, b and t_0 are fitted to the experimental data and the corresponding curve is superimposed in Fig. 4(a) (orange curve). The parameter t_0 corresponds to the time of the asymptotic limit (~ 19 s) where ISI tends to infinity which is often considered to be characteristic of a homoclinic transition [16, 30]. Figure 4(a) also shows that the ISI during a L^S state is not perfectly constant and slightly increases (left hand side insert). This increase is non-linear (like for example in [16]) and seems to become faster close to the transition between L^S and L^{S+1} states. Thus, it appears that this transition is the consequence of a progressive increase of the ISI. It can be noted that this ISI increase during a given L^S state can also be fitted by a function $a + b/(t_0 - t)$ (blue curve in left hand side insert) with different a, b and t_0 than the ones obtained from the fit of the global curve. This behavior was not so clearly marked in Fig. 3(a) due to the smoothing induced by the time window used for calculating the time resolved FFT. Nevertheless, a slight decrease in frequency during each L^S state can be observed on the high order harmonics. As in Fig. 3(b), the duration of each L^S state

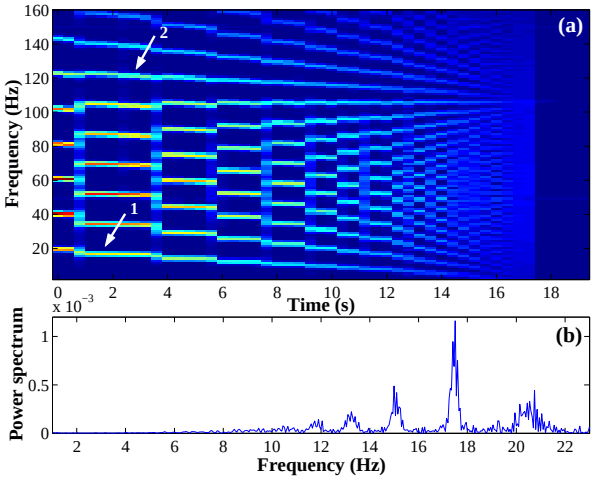

FIG. 3: (color online). (a) Spectrogram of the time series presented in Fig. 2(a). Arrows labeled 1 and 2 show the occurrence frequency of, respectively, spikes and small amplitude oscillations. (b) Power spectral density of the same signal.

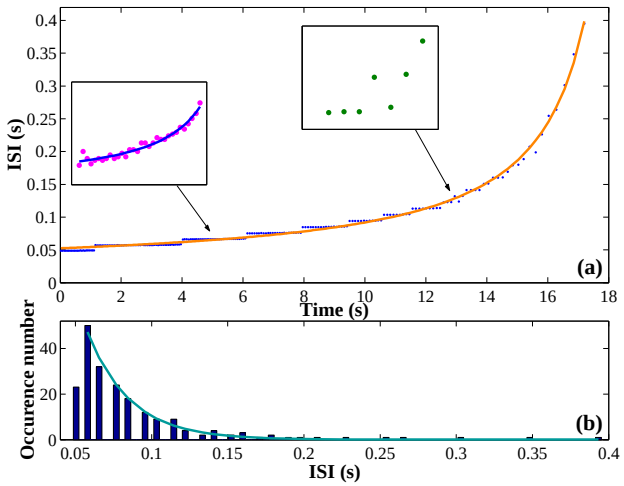

FIG. 4: (color online). (a) Evolution of the ISI during the instability ending phase: measurements (blue dots) and corresponding fit (orange curve). The two inserts are zooms showing, Left: slight evolution of ISI during a L^S phase, Right: unstable transition between two phases. (b) Corresponding histogram of ISIs with an exponential fit (green curve).

can also be analyzed by performing a histogram of ISIs (Fig. 4(b)). This histogram is characterized by a clear multimodal pattern that can be fitted by a decreasing exponential function (green curve, first bar is not taken into account due to missing data as in Fig. 3(b)). Same conclusions can be drawn: when ISI increases, duration of the corresponding state decreases.

This ISI analysis reveals also a particular behavior which is the unstable transition between a L^S and a L^{S+1} state (right hand side insert in Fig. 4(a)). The system changes from a L^S state to a L^{S+1} one but returns to the L^S state once again before changing of state definitively. Experimental observations, not presented here, show that an alternation of two states differing by one failed peak can be observed during several periods. Thus, transitions can take place through the progressive occurrence of L^{S+1} patterns during a L^S state. It suggests that the step-by-step evolution of Fig. 4(a) could be compared to the devil's staircase which is an infinite self-similar staircase structure. This specific structure has been observed in chemistry in the framework of MMOs [9, 10, 12, 31] but also in a wide range of other fields like in physiology [32] or in wave-particle interaction [33]. In chemical systems, this structure is often obtained by representing the firing number $F = L/(L+S)$ as a function of the control parameter. The number of steps is then nearly infinite and in between two parent states, an intermediate state exists with a firing number related to the ones of the parent states by the Farey arithmetic [9, 12, 31]. Thus, the structure obtained in Fig. 4(a) can be an incomplete devil's staircase with an unidentified control parameter evolving with time and not perfectly flat plateaus. More intermediate states could be obtained with a more slowly varying system and thus it can be speculated that the staircase could be partly completed.

In this Letter, we evidenced and characterized mixed-mode oscillations in dusty plasmas. This work highlights new situations of MMOs that can be of interest for improving dynamical system theories related to these structures. The obtained structures are very similar to what is observed in oscillating chemical systems and in neuronal activity. These fields use well-known sets of equations giving rise to MMOs. This scientific background can thus be used to explore and develop new theoretical approaches in dusty plasma dynamics.

M. Lefranc is acknowledged for helpful discussions. The PKE-Nefedov chamber has been made available by the Max-Planck-Institute for Extraterrestrial Physics, Germany, under the funding of DLR/BMBF under grants No.50WM9852. This work was supported by CNES under contract 02/CNES/4800000059.

* Electronic address: maxime.mikikian@univ-orleans.fr

[1] J. Goree, G. E. Morfill, V. N. Tsytovich, and S. V. Vladimirov, Phys. Rev. E **59**, 7055 (1999).
[2] M. Mikikian, L. Boufendi, A. Bouchoule, H. M. Thomas, G. E. Morfill, A. P. Nefedov, V. E. Fortov, and the PKE-Nefedov Team, New J. Phys. **5**, 19 (2003).
[3] K. Avinash, A. Bhattacharjee, and S. Hu, Phys. Rev. Lett. **90**, 075001 (2003).
[4] S. V. Vladimirov, V. N. Tsytovich, and G. E. Morfill, Phys. Plasmas **12**, 052117 (2005).
[5] V. Land and W. J. Goedheer, New J. Phys. **9**, 246 (2007).
[6] M. Cavarroc, M. Mikikian, Y. Tessier, and L. Boufendi, Phys. Rev. Lett. **100**, 045001 (2008).
[7] M. Mikikian and L. Boufendi, Phys. Plasmas **11**, 3733 (2004).
[8] M. Mikikian, L. Couëdel, M. Cavarroc, Y. Tessier, and L. Boufendi, New J. Phys. **9**, 268 (2007).
[9] F. N. Albahadily, J. Ringland, and M. Schell, J. Chem. Phys. **90**, 813 (1989).
[10] V. Petrov, S. K. Scott, and K. Showalter, J. Chem. Phys. **97**, 6191 (1992).
[11] J. L. Hudson, M. Hart, and D. Marinko, J. Chem. Phys. **71**, 1601 (1979).
[12] J. Maselko and H. L. Swinney, J. Chem. Phys. **85**, 6430 (1986).
[13] H. G. Rotstein, T. Oppermann, J. A. White, and N. Kopell, J. Comput. Neurosci. **21**, 271 (2006).
[14] G. Medvedev and Y. Yoo, Physica D **228**, 87 (2007).
[15] J. Rubin and M. Wechselberger, Biol. Cybern. **97**, 5 (2007).
[16] J. Guckenheimer, R. Harris-Warrick, J. Peck, and A. Willms, J. Comput. Neurosci. **4**, 257 (1997).
[17] E. M. Izhikevich, Int. J. Bifurcation Chaos **10**, 1171 (2000).
[18] A. L. Shilnikov and N. F. Rulkov, Phys. Lett. A **328**, 177 (2004).
[19] T. Braun, J. A. Lisboa, and J. A. C. Gallas, Phys. Rev. Lett. **68**, 2770 (1992).
[20] T. Hayashi, Phys. Rev. Lett. **84**, 3334 (2000).
[21] A. Milik, P. Szmolyan, H. Löffelmann, and E. Gröller, Int. J. Bifurcation Chaos **8**, 505 (1998).
[22] J. Guckenheimer and A. Willms, Physica D **139**, 195 (2000).
[23] P. Gaspard and X.-J. Wang, J. Stat. Phys. **48**, 151 (1987).
[24] M. T. M. Koper, Physica D **80**, 72 (1995).
[25] A. P. Nefedov, G. E. Morfill, V. E. Fortov, H. M. Thomas, H. Rothermel, T. Hagl, A. Ivlev, M. Zuzic, B. A. Klumov, A. M. Lipaev, et al., New J. Phys. **5**, 33 (2003).
[26] G. S. Medvedev and J. E. Cisternas, Physica D **194**, 333 (2004).
[27] M. A. Zaks, X. Sailer, L. Schimansky-Geier, and A. B. Neiman, Chaos **15**, 026117 (2005).
[28] A. M. Fraser and H. L. Swinney, Phys. Rev. A **33**, 1134 (1986).
[29] G. S. Medvedev, Phys. Rev. Lett. **97**, 048102 (2006).
[30] U. Feudel, A. Neiman, X. Pei, W. Wojtenek, H. Braun, M. Huber, and F. Moss, Chaos **10**, 231 (2000).
[31] K.-R. Kim, K. J. Shin, and D. J. Lee, J. Chem. Phys. **121**, 2664 (2004).
[32] S. De Brouwer, D. H. Edwards, and T. M. Griffith, Am. J. Physiol. Heart Circ. Physiol. **274**, 1315 (1998).
[33] A. Macor, F. Doveil, and Y. Elskens, Phys. Rev. Lett. **95**, 264102 (2005).